Proceedings of the ASME 2016 International Design Engineering Technical Conferences and Computers and Information in Engineering Conference
IDETC/CIE 2016
August 21-24, 2016, Charlotte, North Carolina

DETC2016-60151

AN EXTENDED PATTERN SEARCH METHOD FOR OFFSHORE FLOATING WIND LAYOUT AND TURBINE GEOMETRY OPTIMIZATION

Caitlin Forinash
School of Mechanical, Industrial, and Manufacturing Engineering
Oregon State University
Corvallis, Oregon, United States
forinasc@oregonstate.edu

Bryony DuPont
School of Mechanical, Industrial, and Manufacturing Engineering
Oregon State University
Corvallis, Oregon, United States
Bryony.DuPont@oregonstate.edu

ABSTRACT

An Extended Pattern Search (EPS) method is developed to optimize the layout and turbine geometry for offshore floating wind power systems. The EPS combines a deterministic pattern search with stochastic extensions. Three advanced models are incorporated: (1) a cost model considering investment and lifetime costs of a floating offshore wind farm comprised of WindFloat platforms; (2) a wake propagation and interaction model able to determine the reduced wind speeds downstream of rotating blades; and (3) a power model to determine power produced at each rotor, and includes a semi-continuous, discrete turbine geometry selection to optimize the rotor radius and hub height of individual turbines. The objective function maximizes profit by minimizing cost, minimizing wake interactions, and maximizing power production. A multidirectional, multiple wind speed case is modeled which is representative of real wind site conditions. Layouts are optimized within a square solution space for optimal positioning and turbine geometry for farms containing a varying number of turbines. Resulting layouts are presented; optimized layouts are biased towards dominant wind directions. Preliminary results will inform developers of best practices to include in the design and installation of offshore floating wind farms, and of the resulting cost and power production of wind farms that are computationally optimized for realistic wind conditions.

INTRODUCTION

The large wind resource off the United States West Coast has the potential to generate wind power for millions of homes, yet the high cost of energy for offshore wind power (compared to traditional sources) has slowed the development of offshore wind farms in the US. By 2030, it is predicted that 54 MW of offshore wind energy will be installed in the US, yet the majority of the proposed projects are for developments off the US East Coast, where the bathymetry is shallow [1]. While the US West Coast has a predicted wind resource totaling over 900 GW, the steep bathymetry and deep waters make it economically infeasible to install embedded, bottom-fixed wind farms [2,3]. Farther off the coast in deep waters, wind speeds are higher and more predictable, and the total resource area is larger [4]. Since bottom-fixed wind installations are not possible, floating wind power installations must be considered.

Floating platforms to support large wind turbines in deep ocean waters are modeled after floating oil and gas rigs [5]. While many types of floating platforms have been proposed, the three main designs are spar-buoy, tension leg-platform (TLP), and semi-submersible. A semi-submersible platform called WindFloat, designed by Principle Power, has been installed off the coast of Portugal, and supports a 2 MW wind turbine [5]. Another project using the WindFloat design, called WindFloat Pacific, is in development off the US West Coast, where a 30 MW array will be installed off the coast of Coos Bay, Oregon [6,7]. However, floating offshore wind installations have high investment and operations and maintenance (O&M) costs that can be prohibitive. Therefore, reducing the cost of floating offshore wind developments is crucial to advancing the floating offshore wind power industry in the United States. While decreasing the initial investment is difficult due to the inherent costs that come with a new floating offshore wind project, it is possible to maximize the profit of a wind farm through means of turbine layout and geometry optimization. This work simultaneously optimizes the turbine layout and geometry of offshore floating wind farms, comprised of WindFloat platforms, using a profit objective.

PREVIOUS LITERATURE: OFFSHORE WIND FARM OPTIMIZATION

Offshore wind farm optimization literature has generally concentrated on bottom-fixed wind farms. Commonly, optimization methods focus on maximizing power output and efficiency of wind farms, with some methods minimizing cost as well. Elkinton et al. developed models that can be applied to any heuristic optimization algorithm for offshore wind farms that maximize power and minimize cost [8,9]. An objective function that minimizes the Levelized Cost of Energy (LCOE) was used, and they found that Genetic Algorithms (GA) and Greedy Heuristic Algorithms were the most viable optimization methods for the offshore wind farm layout problem; however, the models were not applied to an Extended Pattern Search (EPS) method. Pérez et al. also developed a method that can be applied to most optimization algorithms; the two-step sequential procedure combines a heuristic method to set a random initial layout with nonlinear mathematical program techniques that search the space to find local optima [10]. This method was applied to the Alpha Ventus offshore wind farm and, compared to the real layout, increased the Annual Energy Production (AEP) by 3.76%.

Genetic Algorithms (GAs) have been the most common method for offshore wind farm layout optimization; these methods are stochastic, which increase the likelihood of convergence on good solutions in multi-modal systems such as the offshore wind farm layout problem. However, GA's traditionally require the placement of turbines in discrete locations, which limits possible layout combinations. For aligned, staggered, and scattered layout optimization, Gao et al. found that scattered layouts optimized using a Multi-Population GA resulted in the most optimal AEP [11,12]. A model developed by Réthoré et al. included electrical grid and foundation costs as well as energy production [13]. The multi-fidelity model approach that combined 1000 iterations of a Simple GA with 20 iterations of a Sequential Linear Programming method was applied to a case at Middelgrunden Wind Farm in Denmark and was found to limit the computational cost of optimization [13]. Liu and Wang developed an Adapted GA method that replaces the location swaps of traditional GA's with random crossovers; a wind farm containing 16 turbines in a unidirectional, single wind speed case was optimized to 100% efficiency using this method [14].

Additional stochastic optimization methods for multi-modal spaces have been applied to the offshore wind farm layout optimization problem. Rivas et al. developed a Simulated Annealing Algorithm that employed three local search operations; their algorithm increased the AEP of the Horns Rev offshore wind farm by 1% [15]. Using a Coral Reefs Optimization Algorithm, Salcedo-Sanz et al. improved offshore wind farm performance over meta-heuristic algorithms, including Evolutionary Algorithms, Differential Evolution, and Harmony Search [16]. A Viral Based Algorithm with an objective function based on Cost of Energy (COE) was developed by Ituarte et al. that decreased COE for a 30-turbine farm over the layout of Mosetti et al.'s generated using a GA [17].

Rodrigues et al. developed a Covariance Matrix Adaptation Evolutionary Strategy (CMA-ES) in a nested configuration to optimize the layout of a floating offshore wind farm comprised of IDEOL platforms supporting 5 MW turbines [18,19]. This method can optimize layouts in a continuous space for both stationary and moveable platforms. Results from the stationary case showed a decrease in Levelized Production Cost (LPC) of -4.17% over a non-optimized grid layout.

Extended Pattern Search methods have been successfully applied to onshore wind farm layout and turbine geometry optimization [20–23]. The EPS is a moderately stochastic method well-suited for large, multi-modal systems such as the offshore floating wind farm layout and turbine geometry optimization problem. The profit objective used in previous work [20,22,23] informs developers of approximate costs and power production of wind farms, and allows for the inclusion of new models such as a cost model that considers the high costs of offshore floating wind farms comprised of WindFloat floating platforms [5].

PREVIOUS LITERATURE: PATTERN SEARCH

A pattern search algorithm is a deterministic optimization method that searches a space in a set of directions without the use of derivatives. Torczon introduced a class of pattern search methods for optimizing unconstrained nonlinear problems by combining direct search methods [24]. Torczon and Trosset found that, while simplex methods can be unreliable, pattern searches guarantee convergence to a stationary point and can be used when derivatives are unavailable and the objective function is not smooth [25].

Aladahalli et al. introduced a metric for geometric layouts called the sensitivity metric [26]. The sensitivity metric estimates the effect of pattern moves on the objective function, and schedules patterns in decreasing order of their effect on the objective function to increase efficiency. Yin and Cagan explored the effectiveness of different heuristics for generating pattern directions to be used in the pattern search to compare against the coordinate search method [27]. The four methods – conjugate, modified gradient method, rank ordering method, and simplex method – did not significantly improve results but did increase complexity over the coordinate search method.

Vaz and Vicente combined a stochastic particle swarm scheme to increase global convergence with a deterministic pattern search [28]. The pattern search is able to find local minima, while the particle swarm heuristic explores the possible nonconvexity of the objective function to improve global convergence. Cagan presented 3D component layout optimization methods for nonlinear and multimodal spaces, for which deterministic algorithms are unable to navigate [29]. Heuristic rule-based approaches are also not suitable for nonlinear, non-differentiable functions. Therefore, a balance between deterministic and stochastic methods may be ideal, such as the EPS, which combines the deterministic pattern

search with stochastic extensions to increase the likelihood of convergence on good solutions [29].

METHODOLOGY

1. EXTENDED PATTERN SEARCH

EPS methods are ideal for optimizing multi-variable, multi-modal problems by combining a deterministic pattern search algorithm with stochastic extensions. The first two extensions ensure that the EPS traverses in a randomized manner, preventing favoring the selection or movement of any agent. The third extension helps the algorithm avoid stopping at poorly performing local optima. The EPS framework allows for the inclusion of advanced models, such as those used in this work for cost, power production, turbine geometry selection, and wake propagation/interaction. New models can be easily incorporated as technologies for offshore wind farms continue to advance.

The pseudocode given in Fig. 1 shows how the EPS can optimize offshore floating wind systems.

1.1 PATTERN SEARCH

Pattern search algorithms, such as the one incorporated in the EPS used in this work, are a type of direct search algorithm as introduced by Hooke and Jeeves that do not require the calculation of derivatives [30,31]. Pattern search algorithms are deterministic, robust, and computationally inexpensive, but do not perform well alone in multi-modal optimization.

As depicted in the "Pattern Search" box in Fig. 1, the pattern search begins by evaluating the objective function. Then, an agent (in this case, an offshore floating wind turbine) is moved in the first pattern search direction at an initial step size. The objective function is then evaluated again; the move is kept if it has improved the overall objective evaluation. If not, a move at the initial step size is taken in the next pattern search direction. Once an agent is no longer able to accept moves, the pattern search moves onto the next agent in the layout. This process is continued until all agents are no longer moving at the initial step size. Once agents are no longer accepting moves, the step size is reduced and the pattern search begins again. The pattern search is stopped once the step size has been reduced below a user-defined lower bound step size.

1.2 STOCHASTIC EXTENSIONS

Combining stochastic extensions with the deterministic pattern search increases the ability of the algorithm to find better-performing layouts in multi-modal spaces. Yin and Cagan introduced stochastic extensions for three-dimensional component layout optimization that demonstrated increased convergence over a robust simulated annealing algorithm [32]. Three stochastic extensions are included in this work: (1) randomized initial layout, (2) randomized search order, and (3) a popping algorithm. Each extension increases the stochasticity of the EPS.

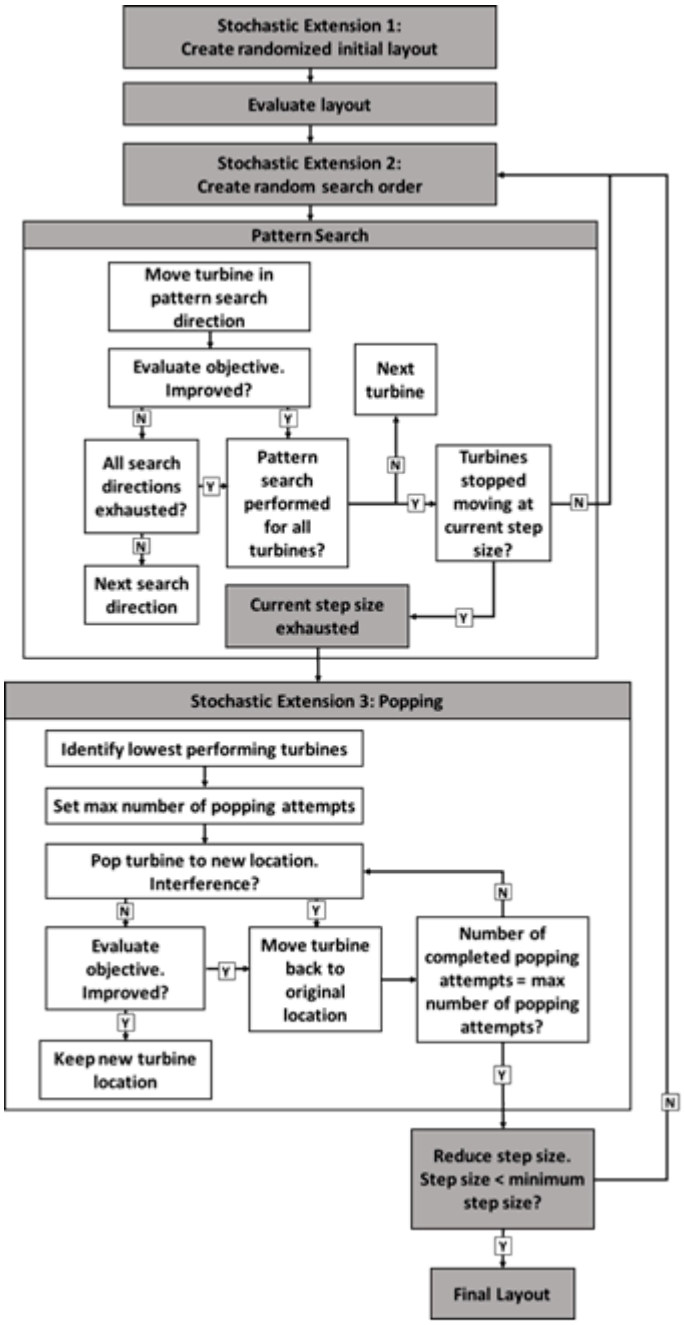

FIGURE 1: EPS PSEUDOCODE

The first stochastic extension occurs only once, at the beginning of the algorithm. An initial layout is created with turbines positioned at randomly-generated locations in the search space. Turbines must be placed at least five rotor radii away from other turbines; otherwise, turbines can be placed anywhere within the search space.

The second stochastic extension occurs at the beginning of each pattern search. The order that the pattern search follows for each turbine is randomly generated for each new step size. This extension reduces the chances of biasing

turbines, since changing the position of individual turbines can affect the power production of surrounding turbines due to changes in wake effects.

The third stochastic extension occurs when the pattern search at each step size has been exhausted. The popping algorithm takes a user-defined number of low-performance agents and "pops" them to new, random locations in the search space. The new, popped locations are evaluated to determine if they improve the overall objective evaluation, and are checked for proximity to other turbines. If the new location improves the objective and is at least five rotor radii from other turbines, the new location is kept. Otherwise, the turbine is moved back to its original location, and popped to new locations until it has found a better location, or a maximum number of popping attempts has been reached.

1.3 OBJECTIVE FUNCTION

This work uses a profit objective function to determine the success of layouts (Eq. 1). The objective function can be used by developers to determine the expected cost and power production of offshore floating wind farms containing a certain number of turbines at a given configuration.

$$Objective = Cost_{total} - (P_{tot} \times c_f \times COE \times t) \quad (1)$$

where $Cost_{total}$ is the total cost of the wind farm (Eq. 2), P_{tot} is the total power produced by the farm (Eq. 13), c_f is the capacity factor, COE is the cost of electricity, and t is the total number of operational hours. Equation (1) is given in negative null form; the objective function is optimized by simultaneously minimizing the total cost and maximizing the total power production.

2. COST MODEL

The cost model developed for this work consists of investment costs and lifetime costs (Eq. 2). Investment costs include capital cost of the turbine and floating WindFloat platform, mooring and anchoring cost, transmission cabling cost, substation cost, and installation cost. The lifetime costs include annual operations and maintenance (O&M) and leasing costs. An in-depth derivation of the cost model is given by Forinash and DuPont [33].

$$\begin{aligned} Cost_{total} &= Cost_{capital} + Cost_{cabling} \\ &+ Cost_{mooring} + Cost_{O\&M} + Cost_{sub} \\ &+ Cost_{installation} + Cost_{operating\ lease} \end{aligned} \quad (2)$$

2.1 TURBINE AND PLATFORM CAPITAL COST

The turbine and WindFloat platform capital cost equation (Eq. 3) is derived from work by Jonkman et al. and Castro-Santos et al. [34,35]:

$$Cost_{capital} = P_{rated,farm} \times \$1.48\ million \quad (3)$$

where $P_{rated,farm}$ is the rated power of the entire wind farm, in megawatts. The rated power of the wind farm is calculated in Eq. (4):

$$P_{rated,farm} = \sum_{i=1}^{N} P_{rated,turbine,i} \quad (4)$$

where $P_{rated,turbine}$ is the rated power of each individual turbine and N is the number of wind turbines in the farm.

2.2 TRANSMISSION CABLING COST

Offshore wind farms require inter-array cabling connecting turbines within the farm, and export cabling to send electricity from the farm to the shore. The cost of inter-array cabling is \$307,000/km (Eq. 5) [36]:

$$C_{inter-array} = d_t \times \$307{,}000 \quad (5)$$

where d_t is the total length of inter-array cabling needed to connect all turbines in the farm, in kilometers. The cost of export cabling is \$484,000/km (Eq. 6) [36]:

$$Cost_{export} = d_s \times \$484{,}000 \quad (6)$$

where d_s is the length of export cabling needed to transport the electricity from the wind farm to an onshore substation, in kilometers.

2.3 ANCHORING AND MOORING COST

The WindFloat platform is connected to the seafloor using four mooring lines attached to drag embedment anchors [37]. The cost of anchoring and mooring are derived from work by Castro-Santos et al. [38,39] and Myhr et al. [36] (Eq. 7):

$$\begin{aligned} C_{mooring} = \\ N \times (\$39{,}772 + \$520{,}820 + \$1{,}096 \times h) \end{aligned} \quad (7)$$

where h is the water depth of the wind farm.

2.4 SUBSTATION COST

This work assumes that an onshore substation would be built for the offshore floating wind project; however, some projects have proposed floating offshore substations. The cost of an onshore substation is calculated based on real renewable energy projects [40] (Eq. 8):

$$Cost_{sub} = \$20{,}000 \times P_{rated,farm} + \$2{,}000{,}000 \quad (8)$$

The base cost of a substation is approximately $2 million, and each additional megawatt adds approximately $20,000 to the total cost of the substation.

2.5 INSTALLATION COST

The cost of installation includes assembling and transporting turbines and platforms to the wind farm site, installing mooring and anchoring, laying transmission cabling, and commissioning [35]. The cost equation relies on the number of turbines to be installed (Eq. 9):

$$C_{installation} = \$977{,}620 \times N \quad (9)$$

2.6 ANNUAL O&M COST

The Jobs and Economic Development (JEDI) Model for Offshore Wind Farms gives an annual cost of O&M equal to $133 per kilowatt of the wind farm [41] (Eq. 10):

$$C_{O\&M} = \$133 \times P_{Rated,Farm} \times y \quad (10)$$

where y is the number of years that the wind farm is operational. O&M must occur at scheduled times, since extreme weather conditions can affect the accessibility of floating offshore wind farms during stormy durations of the year.

2.7 LEASING COST

The Bureau of Offshore Energy Management (BOEM) leases Outer Continental Shelf (OCS) area to developers [42]; leasing and operating fees are calculated using Eq. (11):

$$C_{operating\ lease} = P_{rated,farm} \times 8760 \times c_f \times COE \times r \times y \quad (11)$$

where r is the operating fee rate, equal to 0.02 for the first eight years of operation, and 0.04 every operational year thereafter.

3. POWER MODEL

Power is produced by individual turbines based on the turbine's power curve; turbines of different sizes have different power curves (Fig. 2).

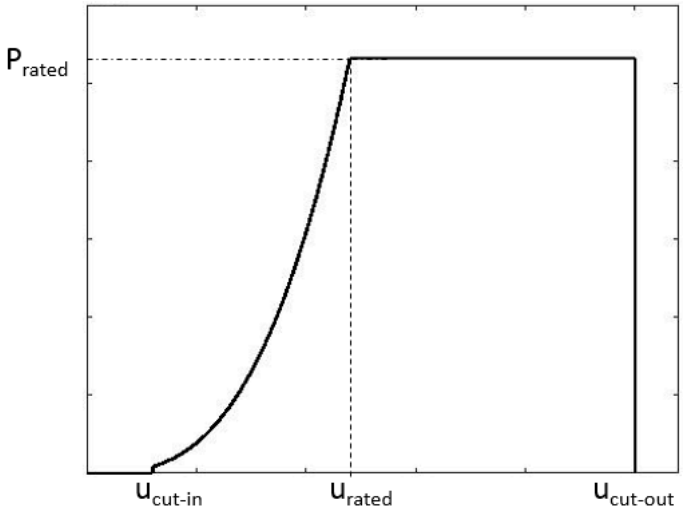

FIGURE 2: WIND TURBINE POWER CURVE

Each turbine model has a cut-in wind speed, rated wind speed, and cut-out wind speed. At wind speeds below the cut-in wind speed, the turbine does not produce power. At wind speeds above the rated wind speed and below the cut-out wind speed, the turbine produces rated power (i.e. nameplate capacity). At wind speeds between the cut-in wind speed and rated wind speed, power production is calculated using Eq. (12) [43]:

$$P = \frac{1}{2}\rho A U^3 C_p \quad (12)$$

where U is the wind speed at the rotor, ρ is air density, A is the rotor swept area, and C_p is the power coefficient. The total power produced by the wind farm is calculated as the sum of the power produced by each turbine (Eq. 13)

$$P_{tot} = \sum_{i=1}^{N} P_i \quad (13)$$

3.1 TURBINE GEOMETRY SELECTION

Wind farms generally consist of a single turbine model; this work considers the possibility of many different models in order to maximize power production and minimize cost by including a turbine size selection within the turbine power production model. Wind turbine geometry selection has been successfully applied to onshore wind farm optimization, resulting in increased power production and improved objective evaluations [20,22,23,44,45]. For each turbine, the optimal turbine size is selected for feasible geometric relationships between rotor radius and hub height, based on commercially available turbines. The turbine geometry selection improves the

overall objective by choosing sizes that maximize power production while minimizing costs; large turbines are able to produce more power, but also have a higher cost. Large turbine sizes are chosen when the wind speed at the turbine's location provides enough power production to overcome the high cost of the turbine. The inclusion of the turbine geometry selection model allows the EPS to choose turbine geometries that optimize layout, rather than imposing an additional constraint of wind turbine size.

4. WAKE PROPAGATION AND INTERACTION MODEL

This work uses a three-dimensional extrapolation of the PARK Wake Model to calculate wind speeds at turbines located in the wakes of upstream turbines [20,46]. As rotating rotor blades of wind turbines extract energy from the wind, a conical wake is created that propagates downstream of the wind direction (Fig. 3).

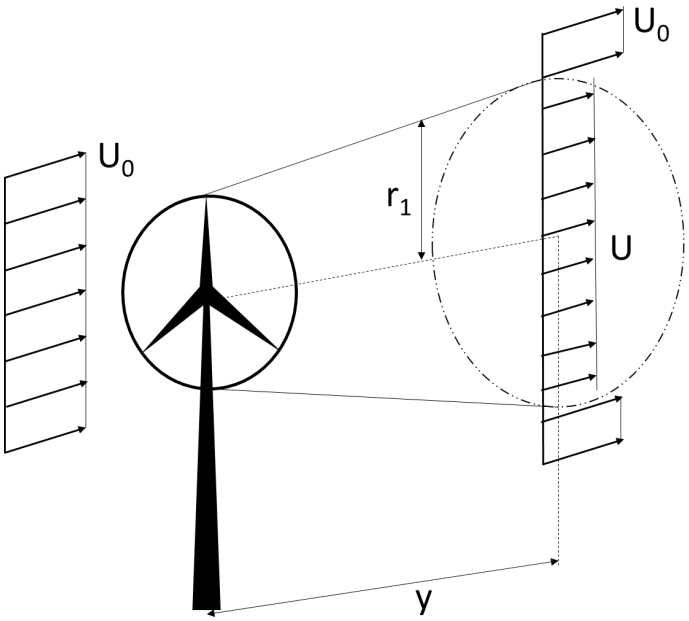

FIGURE 3: THREE DIMENSIONAL WAKE PROPAGATION MODEL

While the wind speed immediately behind the rotor is turbulent and greatly reduced from the ambient wind speed, the wake will eventually disperse and the wind speed will return to ambient. The wind speed downstream of the rotor, U, is calculated using Eq. (14):

$$U = U_o\left[1 - \frac{2}{3}\left[\frac{r_r}{r_r + \propto y}\right]^2\right] \quad (14)$$

where U_o is the ambient wind speed, r_r is the rotor radius of the upstream turbine, y is the distance downstream of the rotor, and $\propto$ is the entrainment constant (Eq. 15):

$$\propto = \frac{0.5}{\ln\left(z/z_0\right)} \quad (15)$$

where z is the hub height and z_0 is the surface roughness. If a turbine's rotor is only partially in a wake, or in multiple wakes, the wind speed is calculated as a summation of the percentage of the rotor radius in each wake (Fig. 4). The equations to calculate the wind speed at rotors with partial and overlapping wakes are derived by DuPont et al. [20,23].

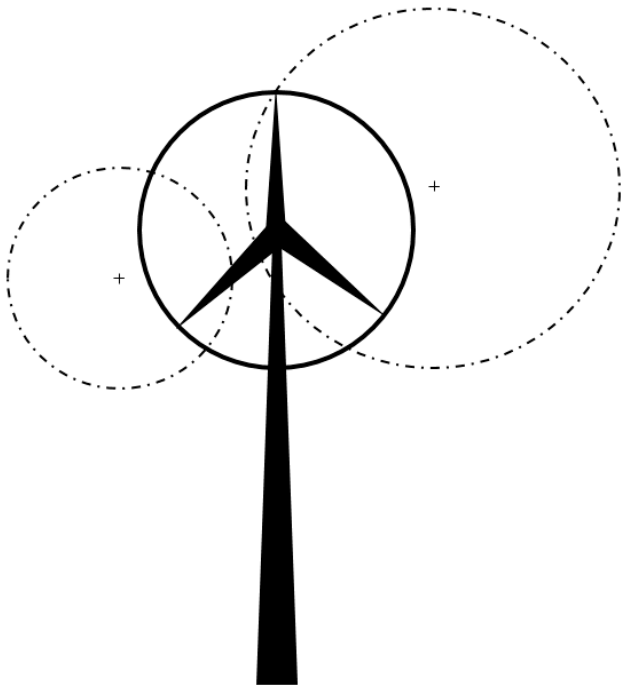

FIGURE 4: INTERACTION OF MULTIPLE WAKES WITH ROTOR SWEPT AREA

PROBLEM FORMULATION

In this work, wind farms are optimized in a square space with side lengths equaling two kilometers. It is assumed that the location is suitable for a wind farm, and there are no constraints on the use of the area. A multidirectional, multiple wind speed wind case is used with three wind speeds and thirty-six wind directions (Fig. 5). The zero-degree onset angle is approaching the bottom of the field, moving clockwise around the field with increasing angles.

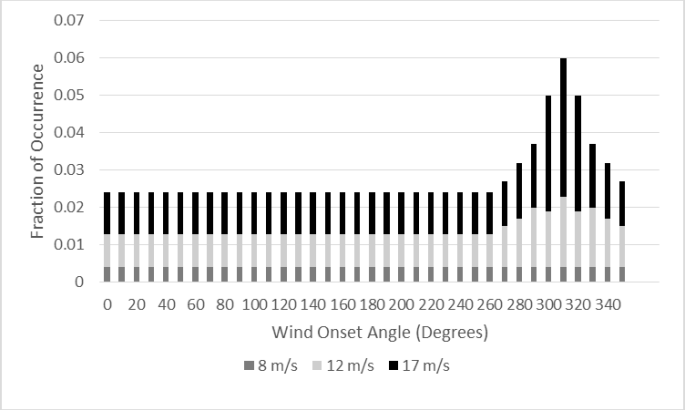

FIGURE 5: WIND ONSET ANGLE AND FRACTION OF OCCURRENCE

Surface roughness of a calm open sea has an empirical value of $z_0 = 0.0002$ meters [43]. The power law exponent, α_h, is equal to 0.11 for most offshore locations and stability conditions [2,47]. The worst-performing 10 turbines are popped in the third stochastic extension; the maximum number of popping attempts is 100. The wind farm is expected to have a 20-year lifetime. The water depth is set to 200 meters, and the distance from shore is set to 30 kilometers. The offshore wind farm optimization parameters are given in Table 1.

TABLE 1: OFFSHORE ENVIRONMENT CHARACTERISTICS

Side length	2000 m
Water Depth	200 m
Life of farm	20 years
Distance from shore	30 km
Surface Roughness	0.0002 m
Power law exponent	0.11
Number of popping attempts	100
Number of popped turbines	10

The study presented in this work explores layouts and turbine geometries optimized for ten sets of wind farms containing one to 22 turbines. The optimal number of turbines for a farm of the size presented subjected to the wind climate presented in Fig. 5 can then be determined, and suggested layouts are presented.

RESULTS

Layouts were optimized using the EPS for farms containing between one and 22 turbines. The objective evaluation for each layout is plotted against the number of turbines in the plot in Fig. 6. Based on the cubic fit with an R^2 value of 0.9026, a minimum objective evaluation occurs when the wind farm contains five turbines. The objective evaluation for the best layout containing five turbines is -\$9.93x10^6 (Fig. 8); the hub height and rotor radius of turbines can be interpreted using the turbine geometry key given in Fig. 7. The average power production for the five-turbine layout is equal to 23.4 MW. The overall minimum objective evaluation for the data shown is equal to -\$1.20x10^7 for a seven-turbine layout (Fig. 9). The average power production for the seven-turbine layout is equal to 28.7 MW.

A 12-turbine layout was generated that also has a low objective evaluation (-\$8.96x10^6, Fig. 10). The average power production of the 12-turbine layout is 42.2 MW.

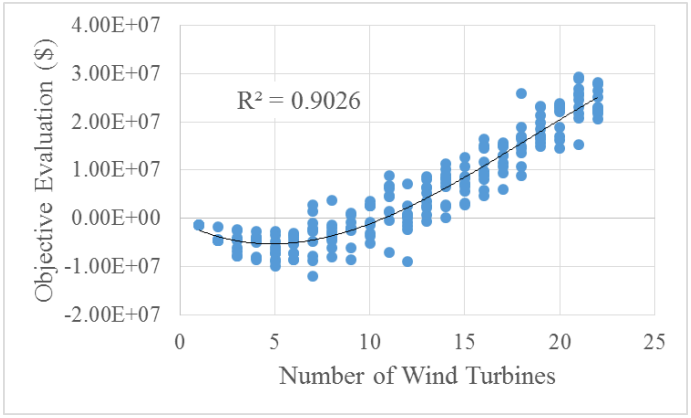

FIGURE 6: OBJECTIVE EVALUATION FOR LAYOUTS CONTAINING ONE TO 22 TURBINES

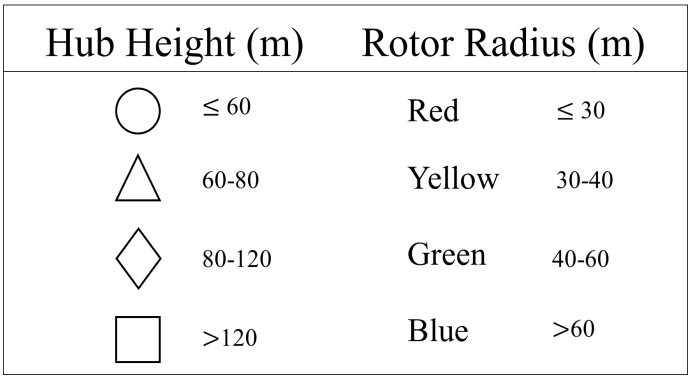

FIGURE 7: TURBINE GEOMETRY KEY

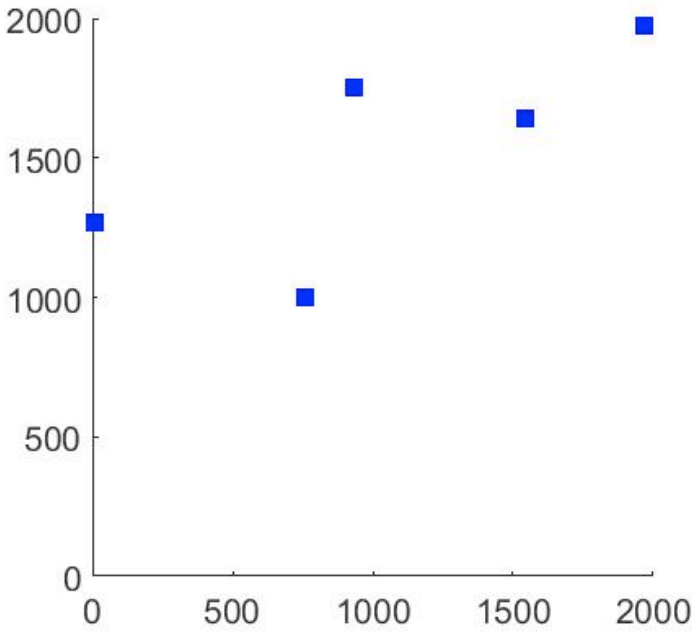

FIGURE 8: OPTIMIZED LAYOUT CONTAINING FIVE TURBINES, OBJECTIVE EVALUATION = -$9.93x10^6

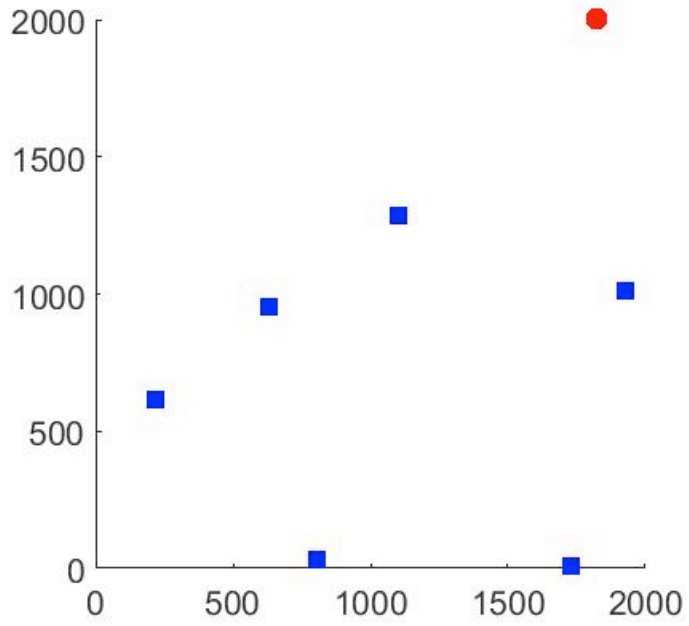

FIGURE 9: OPTIMIZED LAYOUT CONTAINING SEVEN TURBINES, OBJECTIVE EVALUATION = -$1.20x10^7

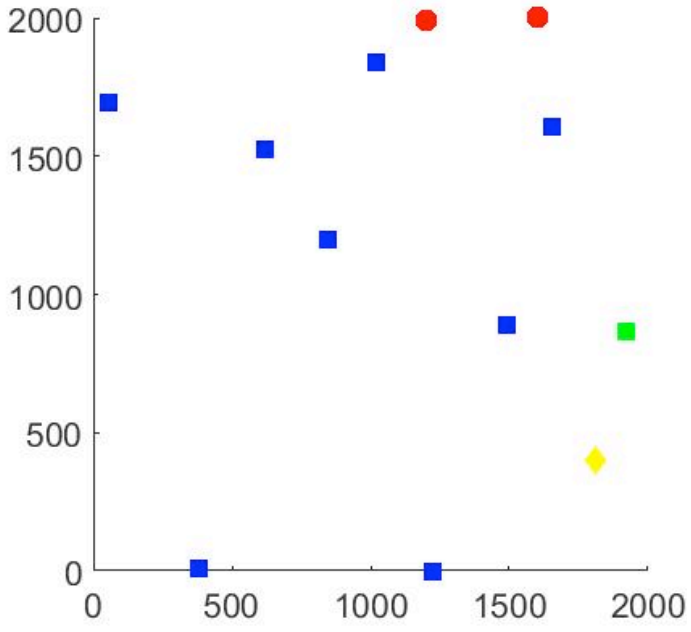

FIGURE 10: OPTIMIZED LAYOUT CONTAINING 12 TURBINES, OBJECTIVE EVALUATION = -$8.96x10^6

DISCUSSION

The layouts given in Figs. 8 and 9 have similar characteristics; turbines line up in perpendicular rows, diagonally across the field, from the bottom left corner to the top right. In the 40° - 60°, and 220° - 240° onset angle wind directions, wake losses are more significant than in other directions. The turbines are lined up perpendicularly to the 310° - 320° wind directions, which experience higher wind speeds at higher frequency (Fig. 5). This means that along the 310° - 320° wind directions where the highest wind energy occurs, wake interactions are minimized; this behavior is expected of optimal layouts. The five-turbine layout shown in Fig. 8 implemented wind turbines of the largest rotor radii and hub heights. This suggests that the power production of each turbine was high enough to overcome the high costs of implementing large turbines. However, the seven-turbine layout shown in Fig. 9 implemented one turbine of the smallest available turbine geometry. It is likely that the EPS did not find a location for this turbine that would allow it to produce enough energy to overcome the high costs, and instead made it as small as possible, both to reduce costs and to help it avoid the wakes of upstream turbines.

The 12-turbine layout shown in Fig. 10 is included to show the behavior of a wind farm containing a higher number of turbines. The 12-turbine layout has some similar behavior as the five and seven-turbine layouts. However, turbines that are not aligned diagonally are placed along the perimeter of the field. This behavior is common among multidirectional wind farm optimization [20,44]. The 12-turbine layout includes four unique turbine geometries ranging in both rotor radius and hub

height. By allowing the EPS to choose the turbine geometry, it is able to further minimize the objective function; if only a single wind turbine hub height and rotor radius were allowed, the resulting layout would have been less optimal than the one shown in Fig. 10.

CONCLUSION

An EPS method for optimizing offshore floating wind energy systems is presented in this work. Turbine layout and geometry are optimized for a 2000-meter square wind farm containing one to 22 turbines. Resulting layouts bias toward dominant wind directions; turbines are placed in rows perpendicular to the dominant wind directions, and along the perimeter of the field.

A cubic fit (with an R^2 value of 0.9026) was applied to the relationship between the number of turbines and the objective evaluations. The minimum occurs for wind farms containing five wind turbines. The overall minimum of the data presented is found for a seven-turbine wind farm; over a life of 20 years, the seven-turbine wind farm is expected to earn $12 million dollars, and have an average energy production of 28.7 MW. The inclusion of the turbine geometry selection model increased the performance of resulting layouts.

Future work will validate the EPS for the multidirectional, multiple wind speed case against multidirectional offshore wind farm optimization results from the literature.

ACKNOWLEDGEMENTS

This work has been funded by Oregon State University.

REFERENCES

[1] Lindenberg, S., Smith, B., and O'Dell, K., 2008, 20% Wind energy by 2030, Washington, DC.

[2] Schwartz, M., Heimiller, D., Haymes, S., and Musial, W., 2010, Assessment of Offshore Wind Energy Resources for the United States, Golden, Colorado.

[3] Sclavounos, P., 2008, "Floating Offshore Wind Turbines," Mar. Technol. Soc. J., **42**(2), pp. 39–43.

[4] Byrne, B. W., and Houlsby, G. T., 2003, "Foundations for offshore wind turbines.," Philos. Trans. A. Math. Phys. Eng. Sci.

[5] Roddier, D., Cermelli, C., Aubault, A., and Weinstein, A., 2010, "WindFloat: A floating foundation for offshore wind turbines," J. Renew. Sustain. Energy, **2**, pp. 1–34.

[6] 2014, "Marine Transmission in Oregon Oregon Department of Energy Marine Transmission in Oregon Marine Transmission in Oregon Report to Oregon Legislature."

[7] Principle Power, 2014, "U.S. Department of Energy Supports Oregon Offshore Wind with Grant Accelerating Development of WindFloat Pacific Project," p. Press Release.

[8] Elkinton, C. N., Manwell, J. F., and McGowan, J. G., 2005, "Offshore Wind Farm Layout Optimization (OWFLO) Project: An Introduction," Optimization.

[9] Elkinton, C. N., Manwell, J. F., and McGowan, J. G., 2008, "Algorithms for Offshore Wind Farm Layout," Wind Eng., **32**(1), pp. 67–83.

[10] Pérez, B., Mínguez, R., and Guanche, R., 2013, "Offshore wind farm layout optimization using mathematical programming techniques," Renew. Energy.

[11] Gao, X., Yang, H., and Lu, L., 2014, "Investigation into the optimal wind turbine layout patterns for a Hong Kong offshore wind farm," Energy, **73**(June 2015), pp. 430–442.

[12] Gao, X., Yang, H., Lin, L., and Koo, P., 2015, "Wind turbine layout optimization using multi-population genetic algorithm and a case study in Hong Kong offshore," J. Wind Eng. Ind. Aerodyn., **139**, pp. 89–99.

[13] Réthoré, P. E., Fuglsang, P., Larsen, G. C., Buhl, T., Larsen, T. J., and Madsen, H. a., 2013, "TOPFARM: Multi-fidelity optimization of offshore wind farms," Wind Energy, (DECEMBER).

[14] Liu, F., and Wang, Z., 2014, "Offshore Wind Farm Layout Optimization Using Adapted Genetic Algorithm: A different perspective."

[15] Rivas, R. A., Clausen, J., Hansen, K. S., and Jensen, L. E., 2009, "Solving the Turbine Positioning Problem for Large Offshore Wind Farms by Simulated Annealing," Wind Eng., **33**(3), pp. 287–297.

[16] Salcedo-Sanz, S., Gallo-Marazuela, D., Pastor-Sánchez, A., Carro-Calvo, L., Portilla-Figueras, A., and Prieto, L., 2014, "Offshore wind farm design with the Coral Reefs Optimization algorithm," Renew. Energy.

[17] Ituarte-Villarreal, C. M., and Espiritu, J. F., 2011, "Optimization of wind turbine placement using a viral based optimization algorithm," Procedia Comput. Sci., **6**, pp. 469–474.

[18] Rodrigues, S. F., Teixeira Pinto, R., Soleimanzadeh, M., Bosman, P. a. N., and Bauer, P., 2015, "Wake losses optimization of offshore wind farms with moveable floating wind turbines," Energy Convers. Manag., **89**, pp. 933–941.

[19] Guérivière, P. de la, 2011, Press Release: IDEOL Announces a New Floating Platform Solution to Accelerate the Deployment of Offshore Wind Farms, La Ciotat, France.

[20] DuPont, B., Cagan, J., and Moriarty, P., 2015, "An Advanced Modeling System for Optimization of Wind Farm Layout and Wind Turbine Sizing Using a Multi-Level Extended Pattern Search Algorithm," Energy, **In Press**, pp. 1–26.

[21] DuPont, B. L., and Cagan, J., 2012, "An Extended Pattern Search Approach to Wind Farm Layout Optimization," ASME J. Mech. Des., **134**, pp. 1–18.

[22] DuPont, B. L., and Cagan, J., 2013, "Multi-Stage Optimization of Wind Farms with Limiting Factors," ASME Int. Des. Eng. Tech. Conf. Comput. Inf. Eng. Conf., pp. 1–12.

[23] DuPont, B. L., Cagan, J., and Moriarty, P., 2012, "Optimization of Wind Farm Layout and Wind Turbine Geometry Using a Multi-Level Extended Pattern Search Algorithm That Accounts for Variation in Wind Shear Profile Shape," Volume 3: 38th Design Automation Conference, Parts A and B, Chicago, Illinois, USA, p. 243.

[24] Torczon, V., 1997, "On the convergence of pattern search algorithms," SIAM J. Optim., **7**(1), pp. 1–25.

[25] Torczon, V., and Trosset, M. W., 1997, "From Evolutionary Operation to Parallel Direct Search : Pattern Search Algorithms for Numerical Optimization," Comput. Sci. Stat., **29**(1), pp. 396–401.

[26] Aladahalli, C., Cagan, J., and Shimada, K., 2007, "Objective Function Effect Based Pattern Search—Theoretical Framework Inspired by 3D Component Layout," J. Mech. Des., **129**(3), p. 243.

[27] Yin, S., and Cagan, J., 2004, "Exploring the Effectiveness of Various Patterns in an Extended Pattern Search Layout Algorithm," J. Mech. Des., **126**(1), p. 22.

[28] Vaz, A. I. F., and Vicente, L. N., 2007, "A particle swarm pattern search method for bound constrained global optimization," J. Glob. Optim., **39**(2), pp. 197–219.

[29] Cagan, J., 2000, "A Survey of Computational Approaches to Three- dimensional Layout Problems," Comput. Aided Des., (412), pp. 1–33.

[30] Hooke, R., and Jeeves, T. A., 1961, ""Direct Search'' Solution of Numerical and Statistical Problems," J. ACM, **8**(2), pp. 212–229.

[31] Torczon, V., 1995, "Pattern Search Methods for Nonlinear Optimization," SIAG/OPT Views News, **6**, pp. 7–11.

[32] Yin, S., and Cagan, J., 2000, "An Extended Pattern Search Algorithm for 3D Component Layout," J. Mech. Des., **122**(1), pp. 102–108.

[33] Forinash, C., and DuPont, B., 2016, "Optimization of Floating Offshore Wind Energy Systems Using an Extended Pattern Search Method," 35th International Conference on Ocean Offshore & Arctic Engineering, In Press, Busan, South Korea, pp. 1–11.

[34] Jonkman, J., Butterfield, S., Musial, W., and Scott, G., 2009, "Definition of a 5-MW reference wind turbine for offshore system development," Contract, (February), pp. 1–75.

[35] Castro-Santos, L., and Diaz-Casas, V., 2014, "Life-cycle cost analysis of floating offshore wind farms," Renew. Energy, **66**, pp. 41–48.

[36] Myhr, A., Bjerkseter, C., Ågotnes, A., and Nygaard, T. a., 2014, "Levelised cost of energy for offshore floating wind turbines in a life cycle perspective," Renew. Energy, **66**, pp. 714–728.

[37] 2011, "WindFloat" [Online]. Available: www.principlepowerinc.com.

[38] Castro-Santos, L., Ferreño González, S., and Diaz-Casas, V., 2013, "Methodology to calculate mooring and anchoring costs of floating offshore wind devices," International Conference on Renewable Energies and Power Quality (ICREPQ)1, Bilbao.

[39] Castro-Santos, L., and Diaz-Casas, V., 2015, "Economic influence of location in floating offshore wind farms," Ocean Eng., **107**, pp. 13–22.

[40] Baker, C., 2015, "Substation Costs."

[41] Lantz, E., Goldberg, M., and Keyser, D., 2013, "Jobs and Economic Development Impact (JEDI) Model: Offshore Wind User Reference Guide," (June).

[42] 2012, Commercial Lease of Submerged Lands for Renewable Energy Development on the Outer Continental Shelf, Herndon, VA.

[43] Manwell, J. F., McGowan, J. G., and Rogers, A. L., 2009, Wind Energy Explained: theory, design, and application, John Wiley & Sons Ltd., West Sussex, UK.

[44] Du Pont, B. L., and Cagan, J., 2012, "An Extended Pattern Search Approach to Wind Farm Layout Optimization," J. Mech. Des., **134**(August 2012), p. 081002.

[45] Chowdhury, S., Zhang, J., Messac, A., and Castillo, L., 2012, "Unrestricted wind farm layout optimization (UWFLO): Investigating key factors influencing the maximum power generation," Renew. Energy, **38**(1), pp. 16–30.

[46] Jensen, N. O., 1983, "A Note on wind generator interaction," Risø-M, p. 16.

[47] Hsu, S. a., Meindl, E. a., and Gilhousen, D. B., 1994, "Determining the power-law wind-profile exponent under near-neutral stability conditions at sea," Am. Meteorol. Soc., pp. 757–765.